Selective resistance to the PARP inhibitor olaparib in a mouse model for BRCA1-deficient metaplastic breast cancer

Linda Henneman[a,1], Martine H. van Miltenburg[a,1], Ewa M. Michalak[a], Tanya M. Braumuller[a,b], Janneke E. Jaspers[a], Anne Paulien Drenth[a], Renske de Korte-Grimmerink[a], Ewa Gogola[a], Karoly Szuhai[c], Andreas Schlicker[d], Rahmen Bin Ali[b], Colin Pritchard[b], Ivo J. Huijbers[b], Anton Berns[e], Sven Rottenberg[a], and Jos Jonkers[a,2]

[a]Division of Molecular Pathology and Cancer Genomics Centre, The Netherlands Cancer Institute, Plesmanlaan 121, 1066 CX Amsterdam, The Netherlands; [b]Mouse Clinic for Cancer and Aging (MCCA) Transgenic Core Facility, The Netherlands Cancer Institute, Plesmanlaan 121, 1066 CX Amsterdam, The Netherlands; [c]Department of Molecular Cell Biology, Leiden University Medical Center, Einsteinweg 20, 2333 ZC Leiden, The Netherlands; [d]Division of Molecular Carcinogenesis, The Netherlands Cancer Institute, Plesmanlaan 121, 1066 CX Amsterdam, The Netherlands; and [e]Division of Molecular Genetics, The Netherlands Cancer Institute, Plesmanlaan 121, 1066 CX Amsterdam, The Netherlands

Edited by David M. Livingston, Dana Farber Cancer Institute, Boston, MA, and approved May 26, 2015 (received for review January 6, 2015)

Metaplastic breast carcinoma (MBC) is a rare histological breast cancer subtype characterized by mesenchymal elements and poor clinical outcome. A large fraction of MBCs harbor defects in *breast cancer 1* (*BRCA1*). As BRCA1 deficiency sensitizes tumors to DNA cross-linking agents and poly(ADP-ribose) polymerase (PARP) inhibitors, we sought to investigate the response of BRCA1-deficient MBCs to the PARP inhibitor olaparib. To this end, we established a genetically engineered mouse model (GEMM) for BRCA1-deficient MBC by introducing the MET proto-oncogene into a BRCA1-associated breast cancer model, using our novel female GEMM ES cell (ESC) pipeline. In contrast to carcinomas, BRCA1-deficient mouse carcinosarcomas resembling MBC show intrinsic resistance to olaparib caused by increased P-glycoprotein (Pgp) drug efflux transporter expression. Indeed, resistance could be circumvented by using another PARP inhibitor, AZD2461, which is a poor Pgp substrate. These preclinical findings suggest that patients with BRCA1-associated MBC may show poor response to olaparib and illustrate the value of GEMM-ESC models of human cancer for evaluation of novel therapeutics.

resistance | mouse model | breast cancer | *BRCA1* | PARP

Poly(ADP-ribose) polymerase (PARP) inhibition provides a promising therapeutic strategy for targeting homologous recombination (HR)-deficient tumors, such as *breast cancer 1* (*BRCA1*)-mutated cancers (1). Indeed, clinical phase I and phase II trials have shown potent anticancer activity of small molecule inhibitors of PARP, such as olaparib, in patients with BRCA1-associated breast cancer (2, 3). However, it remains to be established whether different breast cancer subtypes in *BRCA1* mutation carriers respond equally to PARP inhibition. Reduced sensitivity of breast cancers to anticancer drugs has frequently been associated with an epithelial-to-mesenchymal transition (EMT) (4–7). Metaplastic breast carcinomas (MBCs) are a subset of triple-negative breast cancers (TNBCs) characterized by a claudin-low and EMT-like phenotype (8) and a poor prognosis compared with other TNBCs (9). More than 60% of MBCs have *BRCA1* promoter methylation, raising the question whether these tumors can be effectively targeted by using PARP inhibitors (10). To address this issue in an experimentally controlled setting, we set out to generate a genetically engineered mouse model (GEMM) of BRCA1-deficient MBC by inducing EMT via MET overexpression in a previously established GEMM of *BRCA1*-mutated breast cancer. We report that EMT is associated with olaparib resistance and can be effectively bypassed by administration of AZD2461, a PARP inhibitor with low affinity for the P-glycoprotein (Pgp) drug efflux transporter.

Results

Development of a GEMM-ESC Strategy for Mouse Mammary Tumor Models. GEMMs have the potential to capture the cell-intrinsic and cell-extrinsic factors that drive de novo tumor formation, making them exceptionally valuable for cancer research (11). To speed up the development of novel multiallele GEMMs of human cancer, we previously developed a GEMM-ES cell (ESC) strategy, which permits rapid introduction of mutant alleles into ESCs derived from existing, well-characterized GEMMs and subsequent production of experimental cohorts of chimeric mice that can be directly used for preclinical studies (12, 13). To validate candidate oncogenes and their contribution to therapy resistance in BRCA1-associated breast cancer, we set out to develop a female GEMM-ESC pipeline, based on our *K14cre*;*Brca1*$^{F/F}$;*Trp53*$^{F/F}$ (KB1P) mouse mammary tumor model, in which Cre-mediated stochastic inactivation of BRCA1 and p53 leads to mammary tumors and, to a lesser extent, skin tumors (14). We derived clonal ESC lines from male and female KB1P blastocysts and validated their quality and potency by producing chimeric mice via blastocyst injection (Fig. 1*A*). As expected, sex conversion was evident for the male KB1P clone C3. Clone C3 and female clone A2 contributed well to chimeras, with the majority of animals scoring greater than 40% chimerism, and displayed germ-line transmission. For a second female KB1P clone (C7), more than half of the chimeras showed low chimerism and did not display germ-line transmission, indicating that the quality of this clone was suboptimal (Fig. 1*B*).

Female ESCs tend to undergo XO conversion during in vitro culture. Indeed, copy number variation (CNV) sequencing of female KB1P ESC lines showed loss of one X-chromosome, which was confirmed by whole chromosome painting (Fig. S1 *A* and *B*).

Significance

Poly(ADP-ribose) polymerase (PARP) inhibitors hold promise for patients with *breast cancer 1* (*BRCA1*)-associatated cancers but are anticipated to give rise to resistance. We show that mouse mammary tumors resembling BRCA1-associated metaplastic breast carcinoma display intrinsic resistance to the PARP inhibitor olaparib as a result of increased P-glycoprotein drug efflux transporter expression. These findings may have implications for ongoing clinical trials.

Author contributions: J.J. designed research; L.H., M.H.v.M., E.M.M., T.M.B., J.E.J., A.P.D., R.d.K., E.G., K.S., A.S., R.B.A., and C.P. performed research; I.J.H., A.B., and S.R. contributed new reagents/analytic tools; L.H., M.H.v.M., and A.S. analyzed data; and L.H. and M.H.v.M. wrote the paper.

The authors declare no conflict of interest.

This article is a PNAS Direct Submission.

[1]L.H. and M.H.v.M. contributed equally to this work.

[2]To whom correspondence should be addressed. Email: j.jonkers@nki.nl.

This article contains supporting information online at www.pnas.org/lookup/suppl/doi:10.1073/pnas.1500223112/-/DCSupplemental.

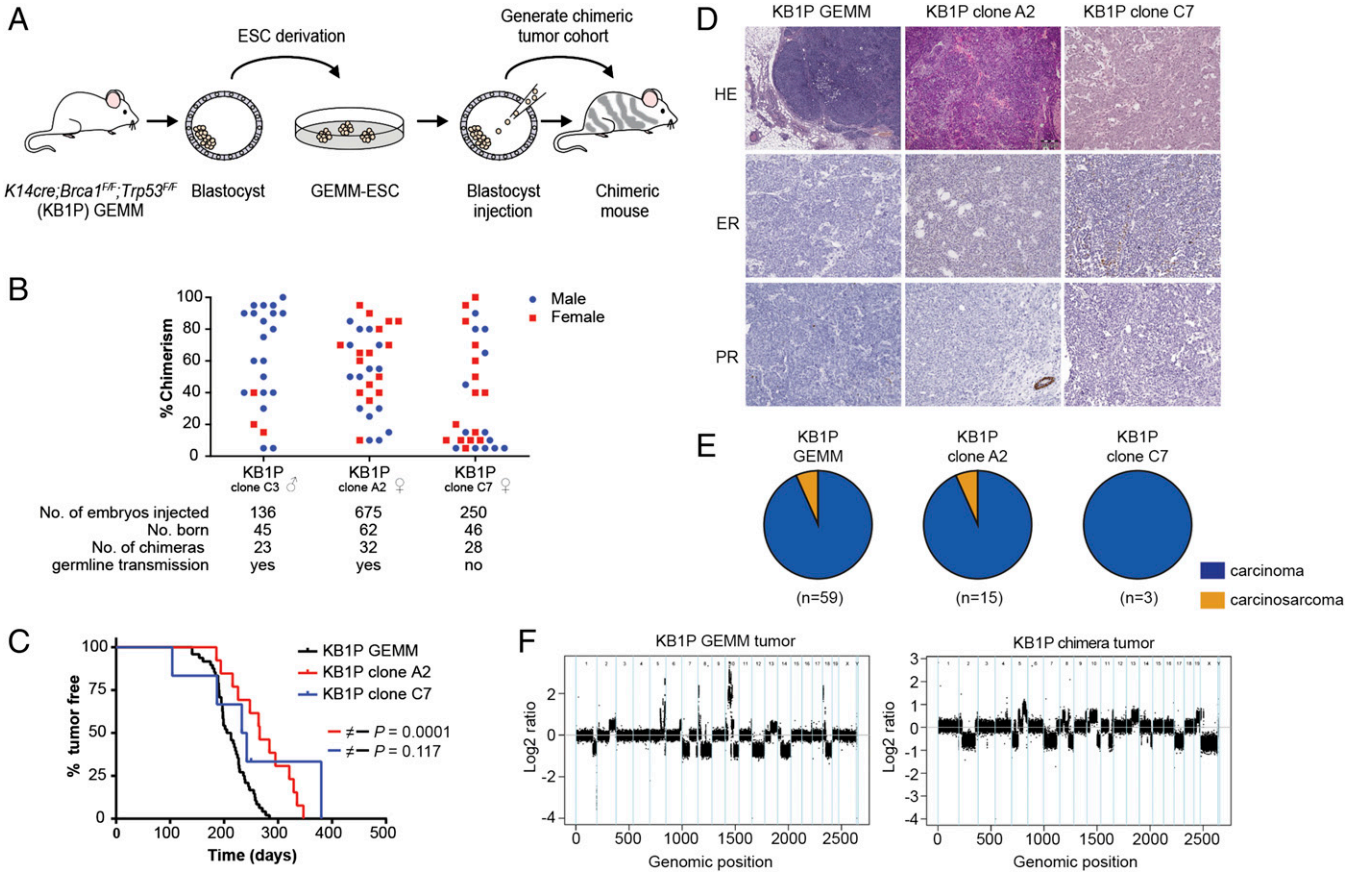

Fig. 1. Mammary tumor development in chimeric mice derived from KB1P ESCs. (*A*) ESCs were isolated from our well-validated KB1P mouse model and subsequently tested for performance to generate chimeric mice. (*B*) Scatter plot showing the performance to generate chimeras of three individual ESC clones (one male, two female). (*C*) Tumor-free survival of KB1P chimeric mice (red, clone A2, t_{50} = 266 d, n = 13 mice; and blue, clone C7, t_{50} = 237 d, n = 6 mice) and KB1P GEMM mice (black; t_{50} = 209 d, n = 48 mice). Log-rank (Mantel–Cox) P value is indicated. (*D*) Histopathology of mammary tumors derived from KB1P chimeric and KB1P GEMM female mice. (*Upper*) H&E staining and (*Middle*, *Lower*) immunohistochemical detection of estrogen receptor (ER) and progesterone receptor (PR). (*E*) Pie diagrams illustrate the distribution of mammary tumor types in KB1P GEMM mice (93% carcinoma; 7% carcinosarcoma) and chimeras from KB1P clone A2 (93% carcinoma; 7% carcinosarcoma) and KB1P clone C7 (100% carcinoma). Carcinomas are shown in blue and carcinosarcomas in orange. (*F*) CNV analysis of KB1P chimeric and KB1P GEMM mammary tumors. Chromosome numbers are represented on the *x* axis and log2 ratio is depicted on the *y* axis.

Previous studies reported that XO mice are viable and fertile but can exhibit some degree of growth retardation, high-frequency hearing loss, reduced thyroid activity, reduced body temperature, and behavioral abnormalities (15, 16). Chimeric mice derived from female KB1P ESCs did not display any abnormalities, were fertile, and gave germ-line transmission, indicating that our female KB1P ESCs contribute to the development of healthy chimeric offspring regardless of their XO status.

Mammary Tumor Development in KB1P Chimeric Mice. Next, we monitored female KB1P chimeras for development of mammary tumors and compared the mammary tumor latency to that of the original KB1P GEMM (Fig. 1*C*). Chimeras of KB1P clone A2 developed tumors with a significantly increased median latency of 266 d vs. 209 d for the original KB1P GEMM ($P < 0.0001$), most likely because of the smaller number of mammary and skin epithelial cells that undergo Cre-mediated loss of BRCA1 and p53 compared with the original model (Fig. 1*C*). There was no significant difference in tumor latency for chimeras of KB1P clone C7, with a median tumor latency time (t_{50}) of 237 d.

Histologically, mammary tumors from KB1P chimeras were estrogen and progesterone receptor-negative and were classified as solid carcinomas, thus showing morphological features comparable to KB1P GEMM tumors (Fig. 1 *D* and *E*). To assess inactivation of BRCA1 and p53 in tumors from KB1P chimeras, we performed Southern blot analysis, which confirmed recombination of the conditional *Brca1F* and *Trp53F* alleles in all cases (Fig. S2). Given that BRCA1 loss leads to genomic instability, we assessed DNA CNVs in mammary tumors from KB1P chimeras by CNV sequencing, which confirmed that KB1P chimeric tumors display genomic instability to the same extent as KB1P GEMM tumors (Fig. 1*F*). Thus, our female GEMM-ESC approach yields healthy chimeras that develop mammary tumors that closely resemble tumors from the original mouse model, and is therefore a novel tool to study breast cancer.

MET Accelerates Mammary Tumor Development in KB1P Chimeric Mice. We next determined if the female GEMM-ESC strategy would be suitable to study the contribution of candidate oncogenes to mammary tumor formation. To allow rapid introduction of additional modifications, we made use of the Flp/FRT recombinase-mediated cassette exchange strategy (13, 17) (Fig. 2*A*). Female KB1P ESC clone A2 was targeted with an FRT homing cassette into the 3′UTR of the *Col1a1* locus to produce *K14cre*;*Brca1*$^{F/F}$;*Trp53*$^{F/F}$;*Col1a1*^{FRT} (KB1P-Col1a1) ESCs (Fig. S3*A*). Next, a Cre-inducible allele of the MET receptor tyrosine kinase, which is associated with EMT and therapy resistance (18, 19), and expressed at high levels in breast cancer (20–22), was introduced in KB1P-Col1a1 ESC clone A2.1 to produce *K14cre*;*Brca1*$^{F/F}$;*Trp53*$^{F/F}$;*Col1a1*$^{inv\text{-}CAG\text{-}Met\text{-}Luc}$ (KB1P-MET) ESCs (Fig. S3*B*). To allow

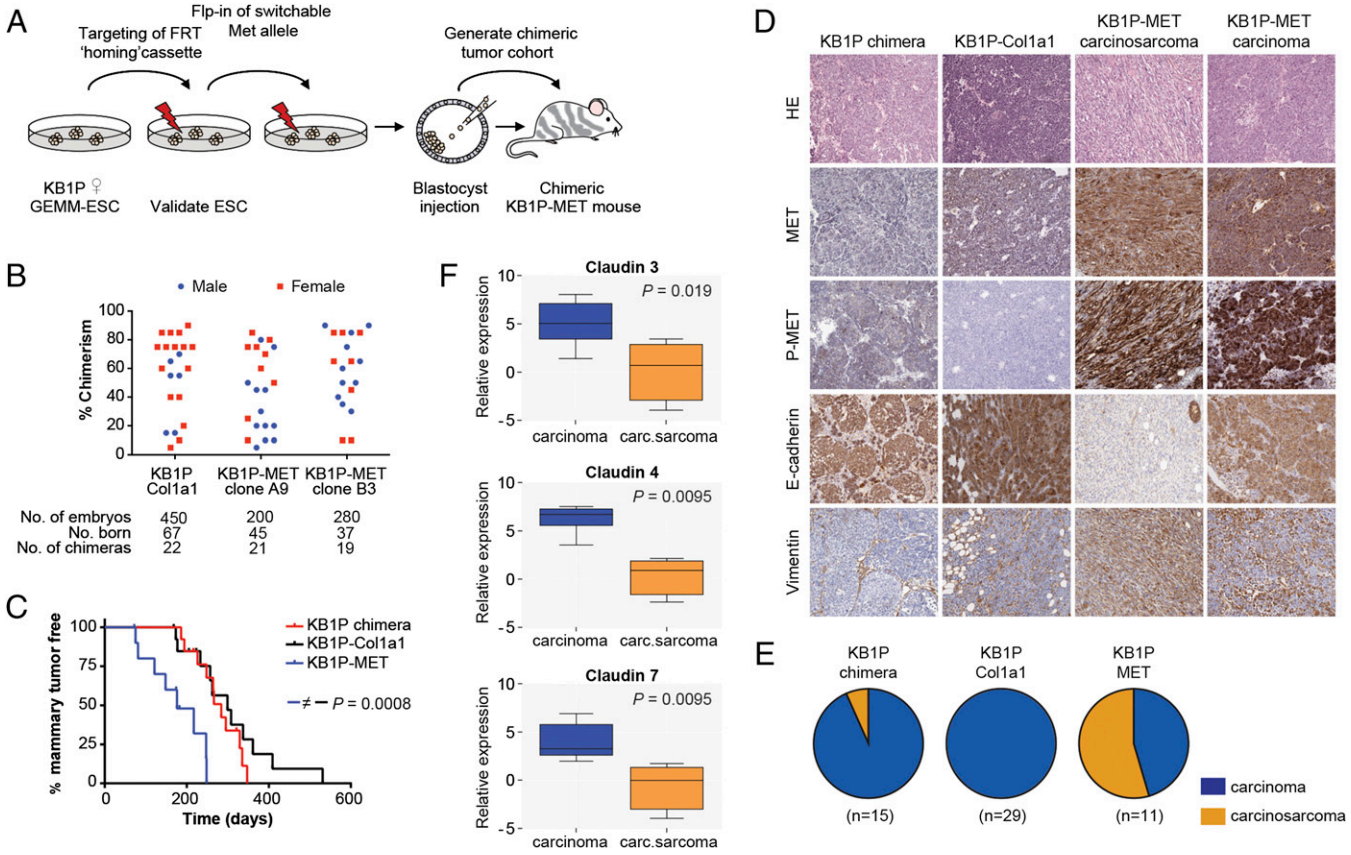

Fig. 2. MET expression in KB1P chimeric mice leads to accelerated mammary tumor development. (*A*) Overview of the experimental procedure. Female ESCs derived from our KB1P mouse model were equipped with a *Col1a1-frt* homing cassette, and subsequently the *Met* proto-oncogene was introduced by recombinase-mediated cassette exchange. (*B*) Scatter plot illustrating the performance of KB1P ESC clones targeted with the *Col1a1-frt* homing cassette (Col1a1), and additionally equipped with *Met* (MET clone A9 and B3) to produce chimeric mice. (*C*) Mammary tumor-free survival of KB1P chimera (red; $t_{50} = 284$ d, $n = 13$ mice), KB1P-Col1a1 (black; $t_{50} = 299$ d, $n = 14$ mice), and KB1P-MET (blue; $t_{50} = 176$ d, $n = 11$ mice) chimeric mice. Log-rank (Mantel–Cox) *P* values are indicated. (*D*) Immunohistochemical staining of formalin-fixed/paraffin-embedded sections from KB1P, KB1P-Col1a1, and KB1P-MET chimeric mammary tumors for H&E, MET, MET$^{Y1234/1235}$, E-cadherin, and vimentin. (*E*) Pie diagrams illustrating the distribution of different mammary tumor types in KB1P (93% carcinoma; 7% carcinosarcoma), KB1P-Col1a1 (100% carcinoma), and KB1P-MET (45% carcinoma; 55% carcinosarcoma) chimeric mice. Carcinomas are shown in blue and carcinosarcomas in orange. (*F*) Box plot showing relative expression of claudin 3, 4, and 7 in KB1P-MET carcinomas and carcinosarcomas. Mann–Whitney *P* values are indicated.

for in vivo monitoring of MET expression by bioluminescence imaging, the *Met* cDNA was fused to a codon-optimized firefly luciferase (*Luc*) gene via an internal ribosomal entry site (Fig. S3*C*). Successful targeting of the FRT homing cassette and subsequent shuttling of the Cre-inducible *invCAG-Met-Luc* construct was confirmed by Southern blot analysis (Fig. S3 *D* and *E*). Luciferase expression was confirmed by bioluminescence imaging of Adeno-Cre–treated KB1P-MET ESCs (Fig. S3*F*). KB1P-Col1a1 and KB1P-MET ESCs produced high-grade female chimeras, which were monitored for mammary tumor development (Fig. 2*B* and Fig. S4*A*). Whereas KB1P and KB1P-Col1a1 chimeras developed mammary tumors with comparable latency, KB1P-MET chimeras developed mammary tumors with a significantly reduced latency of 176 d ($P < 0.001$; Fig. 2*C*), demonstrating that MET overexpression accelerates BRCA1-associated tumor development.

KB1P-MET Chimeras Develop Mammary Tumors with Metaplastic Characteristics. Histopathological analysis revealed that all mammary tumors from KB1P-Col1a1 chimeras were classified as carcinomas. In contrast, more than half of KB1P-MET chimeras developed carcinosarcomas, based on the presence of spindle cells that show E-cadherin loss and vimentin expression, indicating that MET expression promotes the development of metaplastic tumors with an EMT-like phenotype (Fig. 2 *D* and *E*). KB1P-MET carcinosarcomas also showed a claudin-low gene expression pattern, which is a key characteristic of breast cancers with an EMT phenotype (Fig. 2*F*) (8). In contrast to KB1P-MET carcinomas, mice bearing KB1P-MET carcinosarcomas developed tumors with a shorter latency (Table S1), indicating that these metaplastic tumors are more aggressive than carcinomas. Southern blot analysis confirmed Cre-mediated recombination of *Brca1* and *Trp53* in all tumors (Fig. S4*B*).

To confirm that KB1P-MET carcinosarcomas had undergone an EMT, we performed RNA-sequencing and determined the expression level of a panel of EMT signature genes (Fig. S5). KB1P and KB1P-MET tumors clustered perfectly into three groups. KB1P tumors express high levels of epithelial genes; KB1P-MET carcinomas express high levels of epithelial and mesenchymal genes, whereas KB1P-MET carcinosarcomas express high levels of mesenchymal genes. These results show that KB1P-MET mouse carcinosarcomas display an EMT phenotype and, in this respect, resemble BRCA1-deficient MBC in humans (23).

KB1P-MET Carcinosarcomas Display Resistance to the PARP Inhibitor Olaparib. Mammary tumors from GEMMs can be transplanted orthotopically into WT syngeneic female mice while retaining their morphological features, molecular characteristics, and drug-sensitivity profile (24). To confirm that mammary tumors from chimeric mice can be used for transplantation and intervention studies, we orthotopically transplanted 1-mm^3 tumor fragments

from KB1P-Col1a1 and KB1P-MET chimeras into the fourth mammary gland of syngeneic WT female recipient mice. Mammary tumor growth was evident after 4–6 wk and histopathological features of the transplanted tumor outgrowths were preserved, demonstrating that chimera-derived mammary tumors are suitable for allografting.

As MBCs have been associated with therapy resistance and poor outcome (25), we set out to assess if the EMT status of KB1P-MET tumors would affect their response to therapy. When allografted tumors reached a volume of 200 mm^3, tumor-bearing mice were treated with cisplatin (6 mg/kg on days 0 and 14) or olaparib (50 mg/kg daily) for a period of 28 d or until the tumor reached the maximum allowed size of 1,500 mm^3. In line with previous studies (24, 26), KB1P-Col1a1 carcinomas regressed upon cisplatin and olaparib treatment (Fig. 3). Likewise, KB1P-MET tumors shrank upon cisplatin treatment, regardless of their morphological status (Fig. 3*A*). In contrast, whereas KB1P-MET carcinomas regressed upon olaparib treatment, KB1P-MET carcinosarcomas were intrinsically resistant to olaparib (Fig. 3*B*). This suggests that olaparib resistance is not induced by MET expression per se, but rather by MET-associated EMT.

Increased Pgp Expression in KB1P-MET Carcinosarcomas Causes Resistance to Olaparib. Next, we determined if KB1P-MET carcinosarcomas display increased expression of drug efflux transporters, which were previously implicated in olaparib resistance (26). Indeed, we detected increased mRNA expression of the *Abcb1a* and *Abcb1b* genes, both encoding Pgp, in KB1P-MET carcinosarcomas, indicating that these tumors may display resistance by increased efflux of olaparib (Fig. 4*A*). Moreover, *Abcb1a* and *Abcb1b* mRNA levels were strongly correlated to the EMT status of the KB1P-MET tumors (Fig. 4*B*).

To demonstrate that Pgp mediates olaparib resistance of KB1P-MET carcinosarcomas,, we determined the response of KB1P-MET carcinosarcomas to olaparib combined with the Pgp inhibitor tariquidar (XR9576) (27). A KB1P-MET carcinosarcoma with high Pgp expression (donor 2) responded well to the combination therapy, confirming that olaparib resistance is mediated by increased drug efflux by Pgp in this tumor (Fig. 4*C*). Olaparib resistance of a KB1P-MET carcinosarcoma with low Pgp expression (donor 3) could not be bypassed by coadministration of tariquidar, indicating that resistance of this carcinosarcoma was driven by a different mechanism.

Next, we determined the response of KB1P-MET carcinosarcomas to AZD2461, a PARP inhibitor with strongly reduced affinity to Pgp (28). KB1P-MET carcinosarcomas with high Pgp expression (donors 1 and 2) responded well to AZD2461, confirming Pgp-mediated resistance to olaparib (Fig. 4*D*).

To assess whether also human TNBCs with EMT features have elevated Pgp levels, we evaluated *ABCB1* gene expression in several human TNBC subtypes. Similar to mouse KB1P-MET carcinosarcomas and in contrast to basal-like TNBCs with epithelial morphology, the majority of MBCs have a claudin-low phenotype (29, 30). We therefore determined *ABCB1* mRNA levels in claudin-low TNBCs and compared them vs. basal-like TNBCs. As expected, claudin-low TNBCs showed a significantly higher EMT score than basal-like TNBCs (Fig. 5*A*). In addition, claudin-low TNBCs showed significantly increased *ABCB1* mRNA levels compared with basal-like TNBCs (Fig. 5*B*), suggesting that also human MBCs may show intrinsic resistance to olaparib as a result of elevated Pgp-mediated drug extrusion.

Discussion

In this study, we describe a novel female GEMM-ESC strategy for rapid introduction of additional mutant alleles into existing

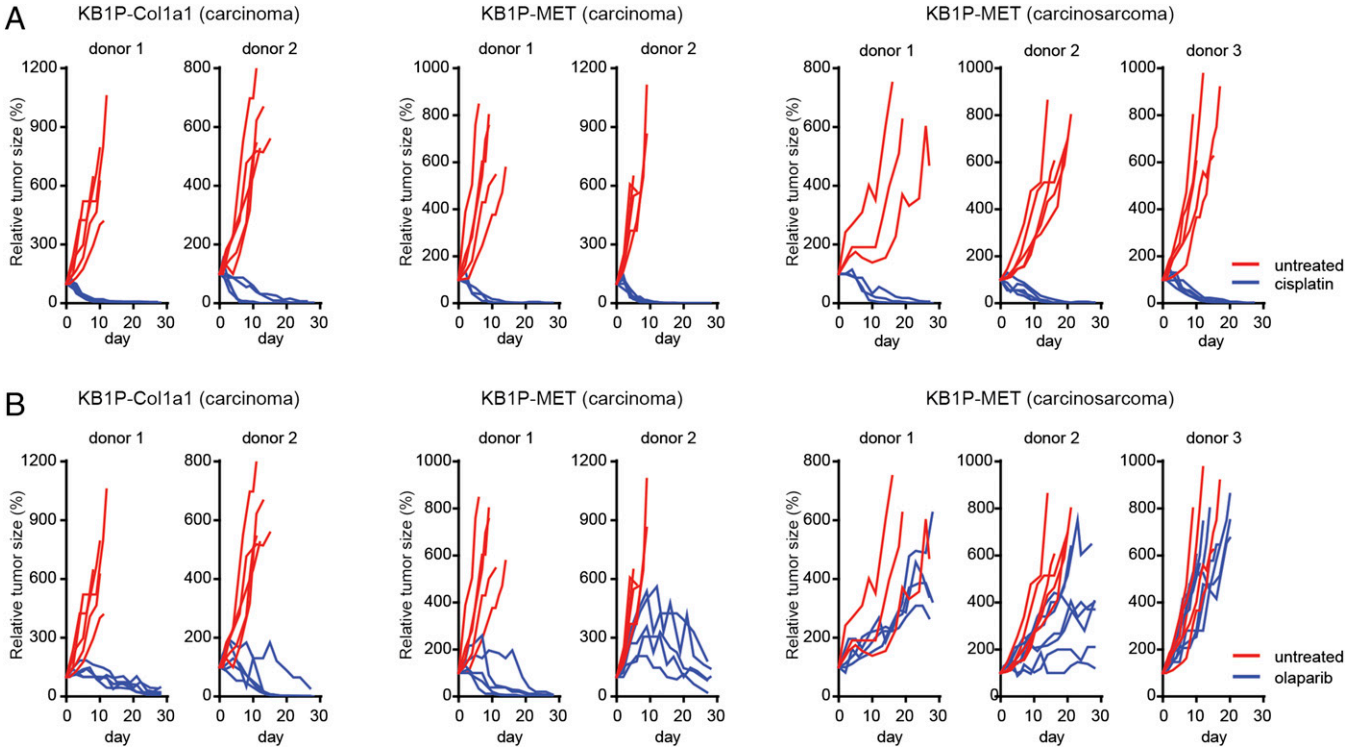

Fig. 3. KB1P-MET carcinosarcomas respond poorly to clinical PARP inhibitor olaparib. (*A*) Small fragments of KB1P-Col1a1 and KB1P-MET epithelial and mesenchymal tumors were transplanted in the fourth mammary fat pad of WT recipient syngeneic mice. When tumors had reached a size of 200 mm^3, mice were treated. Tumor-bearing KB1P-Col1a1 and KB1P-MET mice were treated with 6 mg/kg cisplatin, administered i.v. on day 0 and day 14. Tumor growth was monitored three times per week to assess treatment efficacy. (*B*) Tumor-bearing KB1P-Col1a1 and KB1P-MET mice were treated with 50 mg/kg olaparib daily, administered by i.p. injection, for 28 consecutive days. Tumor growth was monitored three times per week to assess treatment efficacy.

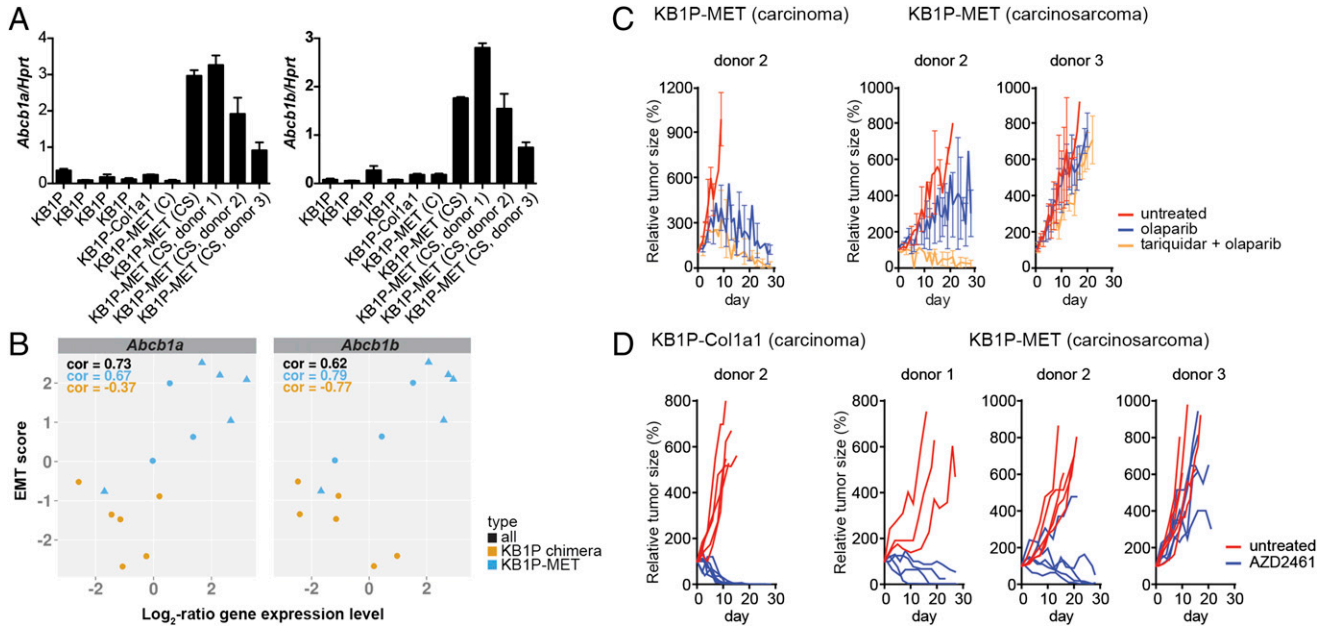

Fig. 4. KB1P-MET carcinosarcomas regress upon AZD2461 treatment. (*A*) Bar graph showing reverse transcriptase-multiplex ligation-dependent probe amplification (RT-MLPA) analysis on mammary tumors from KB1P and KB1P-MET chimeric mice. *Abcb1a* and *Abcb1b* mRNA levels are shown relative to the housekeeping gene *Hprt*. C, carcinoma; CS, carcinosarcoma. (*B*) Scatter plot showing the correlation between EMT status and *Abcb1a* or *Abcb1b* expression levels. Orange circle indicates KB1P chimera; blue circle indicates KB1P-MET carcinoma; blue triangle indicates KB1P-MET carcinosarcoma. (*C*) Small fragments derived from a KB1P-MET carcinoma and two carcinosarcomas were transplanted into the mammary fat pad of WT recipient syngeneic mice. When tumors had reached a size of 200 mm^3, mice were treated with olaparib (50 mg/kg i.p. for 28 d) with or without the Pgp inhibitor tariquidar (2 mg/kg i.p.) or left untreated. Tumor growth was monitored three times per week to assess treatment efficacy. (*D*) Small fragments derived from a KB1P-Col1a1 carcinoma and KB1P-MET carcinosarcomas were transplanted into the mammary fat pad of WT recipient syngeneic mice. When tumors had reached a size of 200 mm^3, mice were treated orally with the PARP inhibitor AZD2461 (100 mg/kg per os for 28 d) or left untreated. Tumor growth was monitored three times per week to assess treatment efficacy.

complex GEMMs of human breast cancer. We also demonstrate the utility of this approach to study cause-and-effect relations in BRCA1-associated breast cancer. An advantage of the female GEMM-ESC approach is that, when female chimeras have been generated, these mice can directly be used for tumor monitoring without further breeding. This strategy effectively reduces time and costs spent on breeding, and—equally importantly—it reduces the total number of mice used to generate a new mouse line. Mammary tumors that develop in chimeric mice derived from GEMM-ESCs are transplantable and therefore suitable for a wide range of preclinical in vivo studies. Moreover, the GEMM-ESC strategy is compatible with CRISPR/Cas9 technology, thus creating a powerful tool for fast-track generation of tailored in vivo models to propel basic and translational cancer research in the era of personalized medicine.

We used the female GEMM-ESC strategy to establish a novel mouse model for *BRCA1*-mutated metaplastic breast cancer by forcing MET expression in our previously established KB1P mouse mammary tumor model. We showed that the resulting KB1P-MET carcinosarcomas are unresponsive to olaparib treatment. Given that EMT is associated with more aggressive breast cancer subtypes (5), it is perhaps not surprising that breast cancer subtypes with mesenchymal elements respond poorly to therapeutics. Notably, several KB1P-MET carcinosarcomas showed elevated levels of the drug efflux transporter Pgp, an observation that was previously reported in olaparib-resistant KB1P tumors (26), but was never linked to their morphological status. In addition, we found elevated *ABCB1* expression in human EMT-like TNBCs with a claudin-low gene expression pattern, suggesting that human BRCA1-deficient MBCs also may display reduced sensitivity to olaparib as a result of Pgp-mediated drug efflux. Interestingly, increased Pgp expression was also associated with olaparib resistance in BRCA2-deficient carcinosarcomas from *K14cre*;*Brca2*$^{F/F}$;*Trp53*$^{F/F}$ mice (31). However, in a KB1P-MET carcinosarcoma expressing low levels of Pgp,

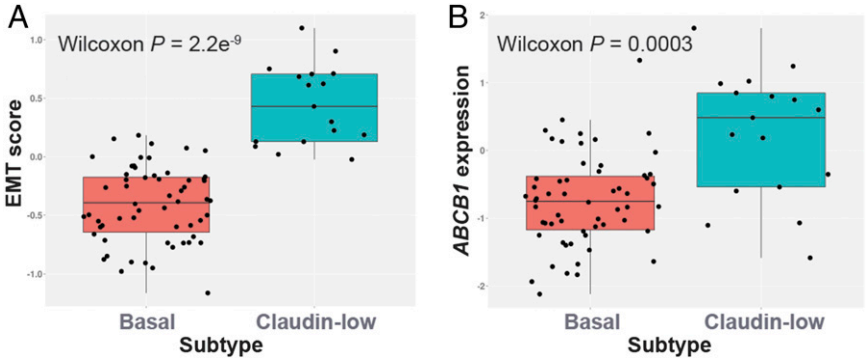

Fig. 5. *ABCB1* expression and EMT score in human basal and claudin-low TNBCs. Box plots showing EMT score (*A*) and *ABCB1* expression levels (*B*) in basal-like and claudin-low TNBCs. Wilcoxon *P* values are indicated.

MEDICAL SCIENCES

unresponsiveness to PARP inhibition could not be explained by drug efflux. This particular tumor (donor 3) showed decreased expression of 53BP1 (Fig. S6*A*), which was previously reported to restore HR and thereby cause olaparib resistance in BRCA1-deficient tumors (24, 25). Indeed, RAD51 foci formation was detected in this tumor following irradiation, suggesting that restoration of HR as a result of 53BP1 loss is the most plausible cause of resistance to olaparib and AZD2461 (Fig. S6 *B* and *C*). We have previously shown that restoration of HR by somatic mutation of *Trp53bp1* encoding 53BP1 occurs in 25% of KB1P mammary tumors with acquired resistance to AZD2461 (28). Whether reduced 53BP1 expression in the AZD2461-resistant KB1P-MET carcinosarcoma is a consequence of MET-induced EMT or caused by (epi)genetic alterations of *Trp53bp1* remains to be determined.

Although clinical phase I and phase II trials have demonstrated anticancer activity of olaparib in patients with BRCA1-associated breast cancer (2, 3), the response of BRCA1-associated MBCs has yet to be established. Our data show that mouse mammary tumors resembling BRCA1-associated MBC display intrinsic resistance to olaparib as a result of increased Pgp drug efflux transporter expression. These preclinical findings may have implications for ongoing clinical trials.

Methods

All animal work was performed in accordance with protocol A11002 approved by the Animal Ethics Committee of The Netherlands Cancer Institute (Amsterdam). Detailed protocols regarding CNV sequencing, whole chromosome painting, Southern blot analysis, targeting ESCs, AdCre infection, bioluminescence imaging, RNA sequencing, EMT signature and human data sets, RAD51 foci analysis, transplantations, histology, and RT-MLPA are described in *SI Methods*.

Antibodies. All antibodies and their dilutions are summarized in Table S2.

Generation of Chimeric Mice. ESCs were derived from KB1P mice and cultured as described previously (13). Male and female ESCs were injected into C57BL/6N blastocysts and implanted into pseudopregnant B6CBAF1/Ola foster mice. The percentage of chimerism of the resulting chimeras was scored by the absence of host-derived coat color. Germ-line transmission was determined by crossing chimeric mice to KB1P (FVB) mice, and the offspring were scored for coat color transmission.

Targeting *Col1a1* Locus and Flip-in of *Met*. Female KB1P ESCs were targeted with the *Col1a1-frt* targeting plasmid followed by Flp-mediated integration of the *frt-invCAG-Met-Luc* vector as described previously (13, 17). Further details are described in *SI Methods*.

ACKNOWLEDGMENTS. We thank the preclinical therapeutics, animal housing and animal pathology cores, and the genomics core facility for their help, and Mark O'Connor (AstraZeneca) for providing olaparib and AZD2461. This work was supported by Worldwide Cancer Research (formerly AICR) Grant 14-0288, Dutch Cancer Society Project NKI-2011-5220, Netherlands Organization for Scientific Research (NWO) NWO-NGI Zenith 93512009 and NWO-VICI 91814643, European Union Seventh Framework Program EurocanPlatform Project 260791, a National Roadmap grant for Large-Scale Research facilities provided by the NWO, Cancer Genomics Centre Netherlands, and the Cancer Systems Biology Center funded by the NWO.

1. Sonnenblick A, de Azambuja E, Azim HA, Piccart M (2015) An update on PARP inhibitors—moving to the adjuvant setting. *Nat Rev Clin Oncol* 12(1):27–41.
2. Tutt A, et al. (2010) Oral poly(ADP-ribose) polymerase inhibitor olaparib in patients with BRCA1 or BRCA2 mutations and advanced breast cancer: A proof-of-concept trial. *Lancet* 376(9737):235–244.
3. Fong PC, et al. (2009) Inhibition of poly(ADP-ribose) polymerase in tumors from BRCA mutation carriers. *N Engl J Med* 361(2):123–134.
4. Hollier BG, Evans K, Mani SA (2009) The epithelial-to-mesenchymal transition and cancer stem cells: A coalition against cancer therapies. *J Mammary Gland Biol Neoplasia* 14(1):29–43.
5. Taube JH, et al. (2010) Core epithelial-to-mesenchymal transition interactome gene-expression signature is associated with claudin-low and metaplastic breast cancer subtypes. *Proc Natl Acad Sci USA* 107(35):15449–15454.
6. Borst P (2012) Cancer drug pan-resistance: Pumps, cancer stem cells, quiescence, epithelial to mesenchymal transition, blocked cell death pathways, persisters or what? *Open Biol* 2(5):120066.
7. Foroni C, Broggini M, Generali D, Damia G (2012) Epithelial-mesenchymal transition and breast cancer: Role, molecular mechanisms and clinical impact. *Cancer Treat Rev* 38(6):689–697.
8. Hennessy BT, et al. (2009) Characterization of a naturally occurring breast cancer subset enriched in epithelial-to-mesenchymal transition and stem cell characteristics. *Cancer Res* 69(10):4116–4124.
9. Jung S-Y, et al. (2010) Worse prognosis of metaplastic breast cancer patients than other patients with triple-negative breast cancer. *Breast Cancer Res Treat* 120(3):627–637.
10. Turner NC, et al. (2007) BRCA1 dysfunction in sporadic basal-like breast cancer. *Oncogene* 26(14):2126–2132.
11. van Miltenburg MH, Jonkers J (2012) Using genetically engineered mouse models to validate candidate cancer genes and test new therapeutic approaches. *Curr Opin Genet Dev* 22(1):21–27.
12. Huijbers IJ, Krimpenfort P, Berns A, Jonkers J (2011) Rapid validation of cancer genes in chimeras derived from established genetically engineered mouse models. *BioEssays* 33(9):701–710.
13. Huijbers IJ, et al. (2014) Rapid target gene validation in complex cancer mouse models using re-derived embryonic stem cells. *EMBO Mol Med* 6(2):212–225.
14. Liu X, et al. (2007) Somatic loss of BRCA1 and p53 in mice induces mammary tumors with features of human BRCA1-mutated basal-like breast cancer. *Proc Natl Acad Sci USA* 104(29):12111–12116.
15. Ishikawa H, Banzai M, Yamauchi T (1999) Developmental retardation of XO mouse embryos at mid-gestation. *J Reprod Fertil* 115(2):263–267.
16. Burgoyne PS, Ojarikre OA, Turner JMA (2002) Evidence that postnatal growth retardation in XO mice is due to haploinsufficiency for a non-PAR X gene. *Cytogenet Genome Res* 99(1-4):252–256.
17. Beard C, Hochedlinger K, Plath K, Wutz A, Jaenisch R (2006) Efficient method to generate single-copy transgenic mice by site-specific integration in embryonic stem cells. *Genesis* 44(1):23–28.
18. Zhang Z, et al. (2014) Functional genetic approach identifies MET, HER3, IGF1R, INSR pathways as determinants of lapatinib unresponsiveness in HER2-positive gastric cancer. *Clin Cancer Res* 20(17):4559–4573.
19. La Monica S, et al. (2013) Gefitinib inhibits invasive phenotype and epithelial-mesenchymal transition in drug-resistant NSCLC cells with MET amplification. *PLoS ONE* 8(10):e78656.
20. Ponzo MG, et al. (2009) Met induces mammary tumors with diverse histologies and is associated with poor outcome and human basal breast cancer. *Proc Natl Acad Sci USA* 106(31):12903–12908.
21. Knight JF, et al. (2013) Met synergizes with p53 loss to induce mammary tumors that possess features of claudin-low breast cancer. *Proc Natl Acad Sci USA* 110(14):E1301–E1310.
22. Zagouri F, et al. (2013) High MET expression is an adverse prognostic factor in patients with triple-negative breast cancer. *Br J Cancer* 108(5):1100–1105.
23. Weigelt B, Kreike B, Reis-Filho JS (2009) Metaplastic breast carcinomas are basal-like breast cancers: A genomic profiling analysis. *Breast Cancer Res Treat* 117(2):273–280.
24. Rottenberg S, et al. (2007) Selective induction of chemotherapy resistance of mammary tumors in a conditional mouse model for hereditary breast cancer. *Proc Natl Acad Sci USA* 104(29):12117–12122.
25. Hennessy BT, et al. (2006) Biphasic metaplastic sarcomatoid carcinoma of the breast. *Ann Oncol* 17(4):605–613.
26. Rottenberg S, et al. (2008) High sensitivity of BRCA1-deficient mammary tumors to the PARP inhibitor AZD2281 alone and in combination with platinum drugs. *Proc Natl Acad Sci USA* 105(44):17079–17084.
27. Mistry P, et al. (2001) In vitro and in vivo reversal of P-glycoprotein-mediated multidrug resistance by a novel potent modulator, XR9576. *Cancer Res* 61(2):749–758.
28. Jaspers JE, et al. (2013) Loss of 53BP1 causes PARP inhibitor resistance in Brca1-mutated mouse mammary tumors. *Cancer Discov* 3(1):68–81.
29. Prat A, et al. (2010) Phenotypic and molecular characterization of the claudin-low intrinsic subtype of breast cancer. *Breast Cancer Res* 12(5):R68.
30. Gerhard R, et al. (2012) Immunohistochemical features of claudin-low intrinsic subtype in metaplastic breast carcinomas. *Breast* 21(3):354–360.
31. Jaspers JE, et al. (2015) BRCA2-deficient sarcomatoid mammary tumors exhibit multidrug resistance. *Cancer Res* 75(4):732–741.
32. Li H, Durbin R (2009) Fast and accurate short read alignment with Burrows-Wheeler transform. *Bioinformatics* 25(14):1754–1760.
33. ENCODE Project Consortium (2012) An integrated encyclopedia of DNA elements in the human genome. *Nature* 489(7414):57–74.
34. Szuhai K, Tanke HJ (2006) COBRA: Combined binary ratio labeling of nucleic-acid probes for multi-color fluorescence in situ hybridization karyotyping. *Nat Protoc* 1(1):264–275.
35. Jonkers J, et al. (2001) Synergistic tumor suppressor activity of BRCA2 and p53 in a conditional mouse model for breast cancer. *Nat Genet* 29(4):418–425.
36. Huang S, et al. (2012) MED12 controls the response to multiple cancer drugs through regulation of TGF-β receptor signaling. *Cell* 151(5):937–950.
37. Kinsella RJ, et al. (2011) Ensembl BioMarts: A hub for data retrieval across taxonomic space. *Database (Oxford)* 2011:bar030.